Phase-Relaxed-Passive Full State Feedback Gain Limits for Series Elastic Actuators

Gray Cortright Thomas, *Member, IEEE,* Joshua S. Mehling, James Holley, and Luis Sentis, *Member, IEEE*

***Abstract*—Full State Feedback (FSF) controllers for Series Elastic Actuators (SEAs) bridge the gap between impedance and admittance controllers. For humanoid robots—which must stably accomplish both stiff and soft behaviors—FSF controllers are ideal candidate joint controllers. However, previous work on FSF gain tuning has used a nonlinear passivity analysis which does not account for time delay and can result in unstable behavior. In this work we introduce a phase-based frequency domain approach to limiting these gains. This strategy can guarantee phase-relaxed passivity according to a relaxation parameter—an a priori bound on the regenerative efficiency of springs appearing in the environment. A simple demonstration illustrates how relaxed phase passivity behaves differently than strict passivity in how it handles the load inertia, allowing stiffness beyond the passive limit.**

I. Introduction

Series Elastic Actuators (SEAs) [1], actuators which are deliberately designed to result in a flexible joint robot [2], have gained widespread adoption for their ability to protect drive-trains from shock loads, allow stable force control, and generate compliant behavior for human–robot interaction. Humanoid robots, in particular, have employed series elastic actuators and have attempted to use them for both impact absorption in the legs, and safely compliant behavior around people.

Typical cascaded SEA control designs [3], [4], [5] are intended to verify stability and passivity for one system with one impedance behavior. However, humanoids and other robots which have reason to switch between extreme impedance behaviors suffer from being locked into a cascaded control structure that prohibits the other extreme behavior [6], [7]. Non-cascaded Full State Feedback (FSF) controllers avoid these structural restrictions, can be shown to generalize some cascaded controllers [8], [9], [10], and fit within LMI design frameworks [11], but pay the cost of greater complexity—making it less obvious how to change the setpoint or impedance.

Originally suggested in [2], a full state feedback control that could place the poles of the feedback linearization of a flexible joint robot (that is, an SEA) was presented in [8]. With an energy-based lyapunov function it was also proven to be passive for a restricted set of gains. In an FSF structure for SEAs, such gain-limiting conditions are critical for ensuring robust coupled stability with the unknown environment. Without these limits we must rely on manual tuning, which restricts the potential to automatically adjust impedance behavior according to a higher level control task. However, the published theoretical limits suffer the drawbacks of being A) merely sufficient conditions and B) only lower bounds with no limit preventing infinite gains [12], [4]. Additional empirical limits (with upper bounds) are recommended in practice [4]. These theoretical results are based on a nominal model which neglects many realistic gain limiting effects, such as time delay, derivative filtering [13], [14], or more generic model uncertainty [15], [16], [17].

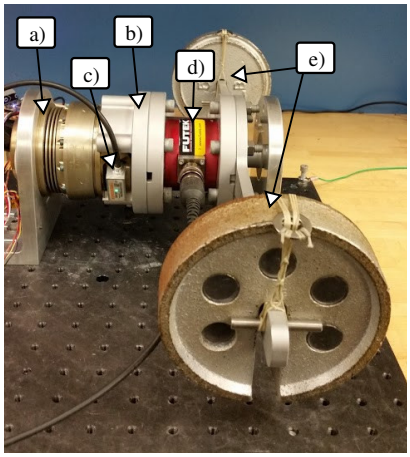

Fig. 1. The experimental testbench, assembled at NASA JSC, comprising: a) an actuator base link (brushless DC motor, harmonic drive transmission, and rotary spring obscured); b) an actuator output link which rotates relative to the base link; c) a spring deflection sensor; d) a calibrated torque sensor; and e) adjustable output inertia (these two weights are tightly lashed to the output lever using high-strength Vectran cable).

To address this gap, we look at the FSF gain limit problem from the perspective of frequency domain design instead of from the traditional nonlinear control perspective. This allows us to model time delay and derivative filtering as we solve the linear systems sub-problem that forms the core of FSF gain limits. Though we do not explicitly treat it here, this problem shows up indirectly even in the multi-joint case [18], [19]. We contribute 1) necessary and sufficient gain conditions for nominal system passivity, 2) gain upper bounds derived from stability and minimum phase aspect of passivity with time delay and derivative filtering 3) a phase-relaxation of passivity that is related to the regenerative efficiency of springs, 4) sufficient conditions for nominal relaxed passivity, 5) a hardware example (see Fig. 1) of a stiffer-than-passive behavior.

This work was supported by NASA Space Technology Research Fellowship grant NNX15AQ33H, "Controlling Robots with a Spring in Their Step," for which G. C. Thomas is the Fellow, L. Sentis is the Advising Professor, and J. S. Mehling is the NASA Advisor.

G. C. Thomas and L. Sentis are with the Mechanical Engineering Department and the Aerospace Engineering Department, respectively, at The University of Texas at Austin, Austin, TX, 78712, USA. (e-mail: gcthomas@ieee.org)

J. S. Mehling is with NASA Johnson Space Center (JSC), 2101 E NASA Pkwy, Houston, TX, 77058, USA.

J. Holley was with NASA JSC. He is now at Celanese Chemical, 9502 Bayport Blvd, Pasadena, TX, 77507, USA.

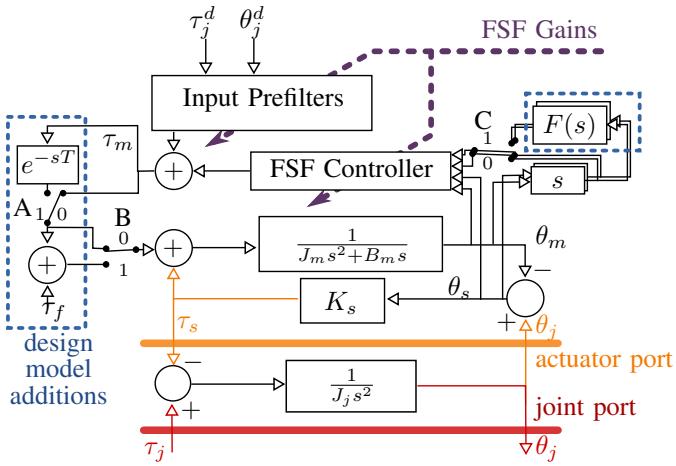

Fig. 2. Nominal model with three design model additions (shown with switches A, B, and C in the off state). If all three are engaged, we have the full design model. With only switch A in the on state, we have the time delay only model. $F(s)$ represents a low pass filter acting exclusively on the two state-derivative inputs to the full state feedback controller. Note that, while the actuator port input is position and output is torque (making the actuator a stiffness), we analyze the system as if the input were torque and the output were position (an integral admittance), like the joint port.

II. Modeling

Our strategy uses two models, shown in Fig. 2. The nominal model is a simplified model that allows for analytical pole and zero placement in the design process. The design model is more complete but less tractable, and is used to justify bandwidth limits on the pole/zero placement process from the nominal model. In both models, there are two non-disturbance inputs (motor torque τ_m and joint torque τ_j) and two (linearly independent) outputs (θ_m and θ_s). These outputs can construct a third output θ_j which is part of the joint port. Drivetrain friction is included in the design model as a bounded disturbance torque, but does not have an impact on stability. The joint inertia J_j is only the modeled part of the inertia, and is not meant to represent perfect knowledge of the environment's inertia. For convenience, the angles, torques, and dynamics are all reflected through the applicable gear ratios into the reference frame of the output.

A. Nominal Model

The frequency domain signals[1] are related as follows in the nominal model:

$$\theta_j = \theta_m + \theta_s, \qquad \tau_j = J_j s^2 \theta_j + \tau_s,$$
$$\tau_s = K_s \theta_s, \qquad (J_m s^2 + B_m s)\theta_m = \tau_s + \tau_m. \tag{1}$$

Defining a full state feedback controller for this nominal model system, we have four states and four parameters (as in other full state feedback controllers [8], [9], [10], [4])

$$\tau_m = -(K_1 + B_1 s)\theta_m + (K_2 + B_2 s)\theta_s, \tag{2}$$

with controller gain variables K_1, B_1, K_2, and B_2. The closed loop integral admittance at the actuator port (Fig. 2),

$$\frac{\theta_j}{\tau_s} = \frac{J_m s^2 + (B_m + B_1 + B_2)s + (K_s + K_1 + K_2)}{(J_m s^2 + (B_m + B_1)s + K_1)K_s}, \tag{3}$$

is second order, with the two poles and two zeros all independently assignable using the four gains. The asymptotic high frequency behavior is the physical spring compliance, and the asymptotic low frequency behavior is $\frac{K_s + K_1 + K_2}{K_1 K_s}$, a feedback gain dependent compliance. The (classical) admittance is simply (3) times s, a non-causal transfer function.

B. Design Model

The design model (Fig. 2) amends the nominal model with the inclusion of three optional confounding factors: A) a time delay on the input τ_m, B) a bounded transmission friction disturbance $|\tau_f| \leq \bar{\tau}_f$, and C) low pass filtering on the derivative signal inputs to the full state feedback controller. This filtering is realistic for the case where no direct velocity sensor is available, and velocity is inferred from a position sensor using a causal filter to approximate differentiation. We parameterize the inclusion of each effect using three Booleans, b_A, b_B, and b_C respectively. This alters the above equations,

$$(J_m s^2 + B_m s)\theta_m = \tau_s + e^{-b_A T s}\tau_m + b_B \tau_f, \tag{4}$$

$$F(s) = \frac{\omega_f}{b_C s + \omega_f}, \tag{5}$$

$$\tau_m = -(K_1 + B_1 F(s) s)\theta_m + (K_2 + B_2 F(s) s)\theta_s. \tag{6}$$

Clearly if all three Booleans are zero, the equations are unchanged from before.

C. Setpoints

Unlike in cascaded systems, changing the setpoint in a full state feedback system is non-trivial [20], [21]. Though it is not part of our experiment, we can invert the closed loop nominal model to find a feed forward motor torque term which will accomplish any 4th order continuous desired joint position trajectory $\theta_j^d(t)$ in the presence of a second order continuous external joint torque trajectory $\tau_j^d(t)$:

$$\begin{aligned}\tau_m = &-(K_1 + B_1 s)\theta_m + (K_2 + B_2 s)\theta_s + \big(K_s^{-1} J_m J_j s^4 \\ &+ K_s^{-1}(B_m + B_1 + B_2) J_j s^3 + K_s^1 (K_s + K_1 + K_2) J_j s^2 \\ &+ J_m s^2 + (B_m + B_1)s + K_1\big)\theta_j^d + K_s^{-1}\big(J_m s^2 \\ &+ (B_m + B_1 + B_2)s + (K_1 + K_2 + K_s)\big)\tau_j^d.\end{aligned} \tag{7}$$

Since the polynomials used are conveniently also the numerator and denominator of the nominal joint integral admittance, any gain conditions that result in nominal joint passivity will naturally also prohibit RHP roots in these feed-forward compensator terms.

D. Transmission Friction

While we do not model any strategies to reduce transmission friction, several exist in the literature already. Ref. [8] suggests a direct friction-model-based compensator. The motor as influenced by the desired current and the spring torque is also a closed system, and any deviation from expected behavior can be canceled by an appropriate friction observer [22], [23], [24], [25]. We include the design model term τ_f in order to draw attention to the following behavior:

Remark 1. In the design model with $b_A = 0$, $b_B = 1$, $b_C = 0$, the sensitivity of torque tracking error (deviation from the nominal model value) to friction torque is

$$\frac{e_\tau}{\tau_f} = \frac{-K_s}{J_m s^2 + (B_m + B_1 + B_2)s + (K_s + K_1 + K_2)}, \tag{8}$$

and therefore is ameliorated if $K_2 + K_1 > 0$, and amplified if $-K_s \leq K_2 + K_1 < 0$.

[1] With notation neglecting functional dependence on the Laplace variable s.

III. Phase-Based Gain Limits

A. Nominal Passivity Limits

The passivity limits of the nominal model can be used to reproduce the simple gain limits from [4]—that

$$K_1, B_1, K_2, B_2 > 0, \tag{9}$$

—since these are are also based on nominal model analysis. In fact, freed from the burden of producing an energy function expression, we can derive necessary and sufficient conditions.

Theorem 1. *The nominal system is passive at the actuator port if and only if*

$$K_1 \geq 0,\ K_2 \geq -K_s + \frac{B_2 K_1}{B_m + B_1},\ B_1 \geq -B_m,\ B_2 \geq 0. \tag{10}$$

Proof. The closed loop actuator port integral admittance defined in (3) is passive iff it has LHP poles and zeros and has phase in the range $[-180°, 0°]$ for all frequencies. LHP poles and zeros occur iff all the coefficients of these second order polynomials are positive (by trivial Routh tests). Thus

$$B_m + B_1 \geq 0,\ K_1 \geq 0, \tag{11}$$

$$B_m + B_1 + B_2 \geq 0,\ K_s + K_1 + K_2 \geq 0, \tag{12}$$

where (11) directly gives two of the conditions. The other two follow from the phase condition. $\angle[\frac{J_m s^2 + (B_m+B_1+B_2)s + K_s + K_1 + K_2}{J_m s^2 + (B_m+B_1)s + K_1}] = \angle[J_m s^2 + (B_m + B_1 + B_2)s + K_s + K_1 + K_2] - \angle[J_m s^2 + (B_m + B_1)s + K_1] \leq 0\ \forall s = j\omega, \omega \geq 0 \iff \pi/2 - \tan^{-1}(\frac{K_1 - J_m\omega^2}{(B_m+B_1)\omega}) \geq \pi/2 - \tan^{-1}(\frac{K_s+K_1+K_2-J_m s^2}{(B_m+B_1+B_2)s})\ \forall\ \omega \geq 0$. This last equivalence uses both $B_m + B_1 \geq 0$ and $B_m + B_1 + B_2 \geq 0$. Since inverse tangent is monotonically increasing, this is equivalent to $-\frac{K_1 - J_m\omega^2}{(B_m+B_1)\omega} \geq -\frac{K_s+K_1+K_2-J_m s^2}{(B_m+B_1+B_2)s}\ \forall\ \omega \geq 0$. This equality holding for all omega is equivalent to it holding for any omega (we will use the limit as $\omega \to \infty$) and the difference $\frac{K_s+K_1+K_2-J_m\omega^2}{(B_m+B_1+B_2)\omega} - \frac{K_1-J_m\omega^2}{(B_m+B_1)\omega}$ having no real roots in ω. The limit condition can be expressed in $\epsilon = 1/\omega \to 0$ as $\frac{J_m - K_1\epsilon^2}{(B_m+B_1)\epsilon} \geq \frac{J_m - (K_s+K_1+K_2)\epsilon^2}{(B_m+B_1+B_2)\epsilon}$ which, neglecting terms of the order ϵ^2 is equivalent to $J_m(B_m + B_1 + B_2) \geq J_m(B_m + B_1) \iff B_2 \geq 0$, the fourth condition in (10). As for the lack of roots, we can rewrite the expression (excluding three special cases: $B_2 = 0$, $B_m + B_1 = 0$, and $B_m + B_1 + B_2 = 0$) as $(B_m + B_1)(K_s + K_2) - B_2 K_1 + \omega^2 J_m B_2$, and therefore $K_2 \geq -K_s + \frac{B_2 K_1}{B_m + B_1}$, the final condition. Returning to the special cases: 1) if $B_2 = 0$, then the test reduces to $\frac{K_s+K_2}{(B_m+B_1)\omega} \geq 0\ \forall\ \omega \geq 0$ and thus $K_2 \geq -K_s$, a special case of this final condition; 2) if $B_m + B_1 = 0$, then returning to the arctangent comparison, and considering in particular the limit as $\omega \to \sqrt{K_1/J_m}$ from below such that $\tan^{-1}(\frac{K_1 - J_m\omega^2}{0\cdot\omega}) = \pi/2 \leq \tan^{-1}(\frac{K_s+K_1+K_2-J_m\omega^2}{B_2\omega})$, we see that $B_2 = 0$, $K_2 \geq K_s$ as before; 3) $B_m + B_1 + B_2 = 0$ forces $B_1 + B_m = B_2 = 0$ which implies case 2. □

These conditions are implied by the sufficient conditions in (9), as expected. They are not convex, and thus do not suggest that gains could be optimized in a tractable convex optimization framework, but they are analytical and therefore easy to check. These bounds are still insufficient to guarantee safety in practice however, because the nominal model omits any factors that would upper bound the gains, and upper bounds are critical for practical stability [4].

B. Passive Phase Limits with Delay

As the following theorem illustrates, passivity is almost incompatible with the design model.

Theorem 2. *With the design model such that $b_A = 1,\ b_B = 0,\ b_C = 0$ it is necessary for actuator port closed loop passivity that*

$$B_2 = 0,\ K_2 = 0,\ \textit{and}\ |B_1| \leq B_m. \tag{13}$$

Proof. For the phase of the actuator port integral impedance $C(j\omega) = N(j\omega)/D(j\omega)$ to be passive, the imaginary part must be negative. Its numerator times the complex conjugate of its denominator must have a negative imaginary part as well. Writing out the expression for $\Im[N(j\omega)\overline{D}(j\omega)]$, we find a third order polynomial in ω with coefficients containing trig functions due to the time delay, we see that the ω^3 term,

$$\omega^3(J_m B_2 \cos(-T\omega)), \tag{14}$$

will both grow to dominate all others at high frequencies and change sign. Therefore for the system to be passive, $B_2 = 0$. Under this condition, the behavior of the ω^2 term is now the dominant term at high frequencies:

$$\omega^2(J_m K_2 \sin(-T\omega)), \tag{15}$$

which similarly necessitates $K_2 = 0$. The final condition comes from the ω term under these conditions:

$$\omega(K_s(B_m + B_1\cos(-T\omega))), \tag{16}$$

which necessitates the final condition. □

This suggests that passivity tests with realistic design models have limited meaningfulness. Nominal model passivity tests mean that realistic design models are likely not themselves passive, but only close—in the sense of model approximation error—to the nominal system which is.

Formally relaxing the phase condition on passivity allows some behavior with clear robotics application that is not permissible in a nominal passivity framework, as we will demonstrate in the section after next.

C. Stability and Minimum Phase

However, these design model additions are well equipped to limit the gains based on the stability and minimum phase requirements of the actuator and even joint integral admittance. By constructing an appropriate test system, a phase margin can confirm that a polynomial or time-delay quasi-polynomial has no roots in the RHP.

Proposition 2. *The actuator port integral admittance is stable and minimum phase for the design model with $b_A = 1,\ b_B = 0,\ b_C = 1$ if the two test systems*

$$\frac{e^{-sT}(B_1 F(s)s + K_1)}{J_m s^2 + B_m s},\ \textit{and}\ \frac{e^{-sT}((B_1+B_2)F(s) + (K_1+K_2))}{J_m s^2 + B_m s + K_s}, \tag{17}$$

are stable under unit negative feedback.

Proof. These test systems are designed to have closed loop denominators equal to the numerator and denominator, respectively, of the actuator port integral admittance (similar to (3), but for the design model). □

There are various ways of relating this condition to the gains which are involved but not novel (e.g. the Bode plot phase margin test). This is how we upper bound the gains.

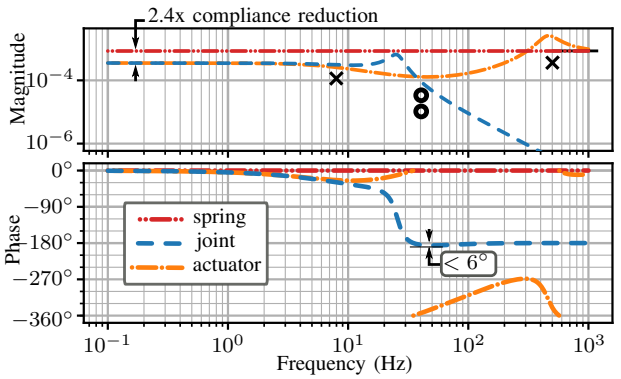

Fig. 3. Bode plot of a FSF tuning beyond the passive stiffness limit with the design model ($b_A = 1,\ b_B = 0,\ b_C = 1$), showing the closed loop design model actuator port integral admittance (—•—) and joint port integral admittance (— —). For comparison, the integral admittance of the physical spring is shown (••—••). The nominal model's poles and zeros of actuator port integral admittance are marked in black (poles as X, zeros as O).

IV. Relaxing Passivity using Phase

Definition 1 (Regenerative Efficiency)**.** Consider a passive linear system with derivative impedance (reciprocal of integral admittance) $S(j\omega)$ engaged in steady state sinusoidal behavior at angular frequency Ω, with position $\theta(t) = a_0\cos(\Omega t)$ and torque $\tau(j\omega) = S(j\omega)\theta(j\omega)$. We name the energy $E_r = -\int_0^{\frac{\pi}{2\Omega}} \dot\theta(t)\tau(t)dt$ the *recovered* energy harvested as the system moves from a_0 to rest. Similarly, $E_i = \int_{\frac{\pi}{2\Omega}}^{\frac{\pi}{\Omega}} \dot\theta(t)\tau(t)dt$ is the *input* energy required to displace the system from rest to $-a_0$. If the system is an ideal spring, these energies are the same. We define the energy ratio $\eta(S,\Omega) = \frac{E_r}{|E_i|}$, as the *spring-mode regenerative efficiency* at this frequency.

Proposition 3 (ψ-Restricted-Phase Passive Systems)**.** *The spring-mode regenerative efficiency $\eta(S,\Omega)$ for a passive linear system that has a derivative impedance $S(j\omega) = S_r(\omega) + jS_i(\omega)$ with $\angle S(j\omega) \in (\psi,\ \pi)\ \forall\omega$ for the phase restriction parameter ψ, $0 \le \psi \le \pi/2$, which we term a ψ-restricted-phase passive system, is bounded:*

$$\eta(S,\Omega) = \frac{2S_r(\Omega) - \pi S_i(\Omega)}{|2S_r(\Omega) + \pi S_i(\Omega)|} < \frac{2\cos(\psi) - \pi\sin(\psi)}{|2\cos(\psi) + \pi\sin(\psi)|}\ \forall\ \Omega. \quad (18)$$

Proof. Equality follows from substituting $\tau(t) = S_r(\Omega)a_0\cos(\Omega t) - S_i(\Omega)a_0\sin(\Omega t)$ and directly computing the efficiency $\eta(S,\Omega)$. Inequality bound results from a monotonic relationship within the specified angle range. □

Proposition 4 (ψ-Relaxed-Phase Passivity)**.** *We call a system whose integral admittance is stable, minimum phase, and has phase within the range $[-\pi - \psi, 0]$ a ψ-relaxed-phase passive system. The feedback interconnection of a ψ-relaxed-phase passive system and a ψ-restricted-phase passive system is stable for all $0 \le \psi \le \pi/2$.*

Proof. By the Nyquist criterion: the phase of the (stable) open loop system is restricted to $(-\pi, \pi)$, thereby preventing its Nyquist plot from reaching or encircling the -1 point. □

V. Nominal Relaxed Passivity at the Joint Port

The ψ-phase-relaxed passivity of the nominal model's joint port can now be used to derive more permissive gain limits.

Theorem 3. *If the gains satisfy* (11), (12)*, and there exists a "certificate angular frequency" ω_c such that*

$$B_2 \ge -\frac{(B_m + B_1)(K_s + K_2)}{J_m\omega_c^2 - K_1},\quad K_2 \ge -K_s + \frac{B_2K_1}{B_m + B_1},$$

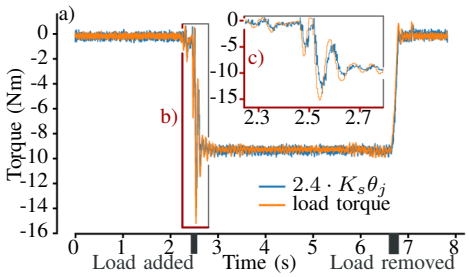

Fig. 4. Comparison of measured and expected stiffness behavior. An off-center weight is placed on the device and then removed to generate a pulse-like torque profile. Measured deflection θ_j is amplified by the expected low frequency stiffness to show that it matches the measured load torque τ_j. This torque follows a spring behavior 2.4 (i.e. $\frac{K_1}{K_1+K_2+K_s}$) times stiffer than the series spring, indicating a stiffness beyond the passive limit. From the large scale graph a), region b) is expanded for clarity in sub-figure c).

$$K_1^2\omega_c^{-4} - 2\frac{J_mK_1}{\omega_c^2} + J_m^2 + \frac{(B_1+B_m)^2}{\omega_c^2} \le +J_j[((K_1+K_2 +K_s) - J_m\omega_c^2)^2 + (B_1+B_2+B_m)^2\omega_c^2](\tan^{-1}(\psi))^2, \quad (19)$$

then the nominal system is ψ-relaxed-phase passive at the joint port.

Proof. The first two conditions are sufficient to guarantee that the phase of the actuator port integral admittance is in the passive range $\forall\omega\ :\ 0 \le \omega \le \omega_c$, and therefore so is the phase of the joint port integral admittance. The final condition claims that the actuator port integral admittance magnitude is at least $1/\tan^{-1}(\psi)$ times the magnitude of the integral admittance of the joint inertia alone. Since the LHS terms are positive and decreasing with ω_c and RHS terms are positive and increasing with ω_c, the inequality holds for all $\omega > \omega_c$. With this magnitude relationship, we can guarantee the difference between the joint port integral admittance phase and the phase of the joint inertia integral admittance is less than ψ and therefore satisfies the relaxed phase passivity criteria. Inequalities (11) and (12) guarantee that the nominal actuator admittance is stable and minimum phase. The joint port admittance has the same numerator, and the roots of its denominator are guaranteed to be LHP because ω_c is also higher frequency than the crossover frequency of the product system of actuator port integral admittance and J_js^2 under unit negative feedback, and the phase condition guarantees that this feedback results in a non-negative phase margin. □

Note that these conditions only ensure *ψ-relaxed-phase passivity* at the *nominal* model's *joint* port. An analytical expression for ψ-relaxed-phase passivity of the design model's joint port is beyond the scope of this paper. However, if (11) and (12) hold, the relaxed phase condition can be graphically verified after the fact using the Bode plot of the design model's joint port's integral admittance (see Fig. 3).

VI. Experiments

Using a NASA Valkyrie actuator (Fig. 1, [26]) we demonstrate the behavior of the controller from Fig. 3.

A. System Identification

We identify the parameters of our linear model (Tab. I) using closed loop tests driven by the joint output (and not by the motor, as is more typical). This testing scheme makes use of the assumed model structure for a series elastic actuator.

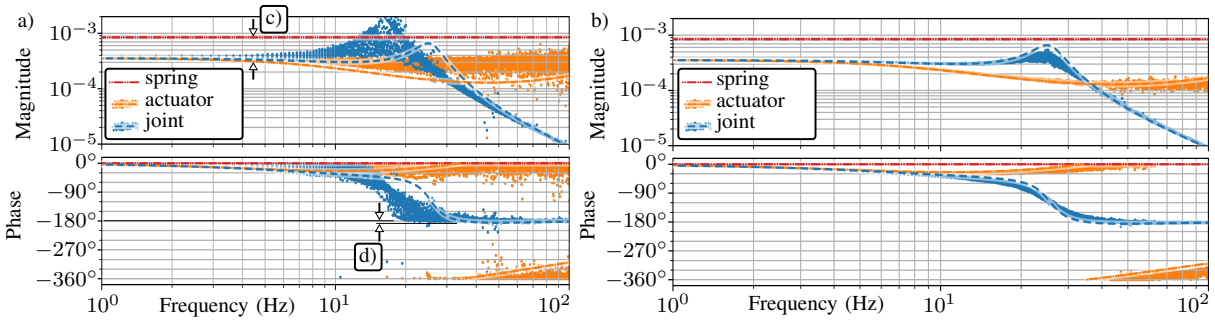

Fig. 5. Demonstration of FSF tuning beyond the passive stiffness limit. Bode plots show integral admittance transfer functions (position over force) for the passive spring ( ), the actuator port (, and data dots of the same color), and the joint port (, and dots of the same color)—which is inferred from the actuator behavior and the joint inertia. Subplot a) shows the raw frequency domain measurements (dots) from 20 experiments using the same controller. Subplot b) shows the same data with a compensatory term that eliminates friction and other errors in the motor model (i.e. corrected motor position is found as a transfer function of the difference between motor torque and spring torque). Joint and actuator port integral admittance show a clear reduction (c) relative to spring compliance at low frequencies—indicating the stiffness is beyond the passive limit. Joint port integral admittance does not violate the phase-relaxed passivity criteria (d).

The first test has no feedback controller. From the empirical integral admittance of the motor, $\hat{\theta}_m/\hat{\tau}_s$, we find a linear estimate for the reflected motor damping, B_m. The second test finds the negative motor velocity feedback which corresponds to the boundary of stability using bisection search. Assuming the motor velocity feedback has canceled the motor damping, we estimate the motor torque constant. Using this controller, we measure a new estimate of the closed loop motor integral admittance. From this we find an estimate of the reflected motor inertia, J_m. Third, we design a stiff motor position controller. Exerting force on the output again, we measure an empirical estimate of the spring stiffness by comparing the spring deflection with the output torque sensor. Fourth and finally, we attach the joint inertia load and drive the system from the actuator side instead of the load side. (To do this, we attach a lever arm fixture to the motor housing, and excite manually as in the other tests.) The torque on the load from the actuator is equal and opposite to the torque on the actuator from the load, so we use the negative of the load cell measurement. The empirical joint integral admittance thus reveals J_j, and our identification is complete.

B. Frequency Domain Results

As shown in Fig. 5, the controller of Tab. I achieves a lower joint integral admittance than the compliance of the series spring. The bode plot also reveals that the controller results in a non-passive actuator integral admittance. The experimental bode plots are truncated to 100 Hz due to the low signal to noise ratio above this frequency. Each one overlays 20 tests to show the variation in the results.

The two bode plots in Fig. 5 differ in that Fig. 5.b corrects (post-hoc) for τ_f using an offline disturbance estimator. Fig. 5.b which is far closer to our expectation, which suggests that the drivetrain friction is the reason that our engineered damping ratio does not appear in the raw bode plot Fig. 5.a.

C. Time Domain Results

Time domain results can only show interaction with a single environment, and are therefore only able to falsify passivity or relaxed passivity claims, but they are relatively easy to interpret. Fig. 4 shows how similar the resulting actuator stiffness is to an ideal spring 2.4 times higher than the series elastic spring. It also demonstrates some high frequency error in the result which could be counted as the main drawback of such an aggressive control technique. It seems that there is even some periodicity to the error. A small amplitude oscillation is noticeable at roughly 15 Hz, corresponding with the large resonant peak seen in the joint integral admittance of Fig. 5.a. This frequency matches the resonant frequency of the added inertia and the ideal stiffness the actuator is simulating. The persistence of the oscillations means the system is sustaining them energetically (contrary to the claims of the analysis), but the fact that the oscillations at the transition die out indicates that the oscillation magnitude is stable. Thus these oscillations are probably due to an unmodeled nonlinearity (e.g. the motor damping properties changing at small amplitudes due to Coulomb friction) that compromises the passivity guarantee for small amplitude, but not large amplitude, deviations from the equilibrium. This non-passivity at low amplitudes allows the system to keep this resonance going by injecting energy at the joint port.

TABLE I
PARAMETERS OF THE ACTUATOR AND CONTROLLER

Parameter	Value	Gain	Value
J_m	0.44 Kg m^2	K_1	69,480 Nm/rad
B_m	17.9 Nm s/rad	B_1	1,387 Nm s/rad
K_s	1 180 Nm/rad	K_2	-41,690 Nm/rad
J_j	0.29 Kg m^2	B_2	-1,183 Nm s/rad

VII. CONCLUSION

This paper applies frequency domain thinking to the problem of gain limits in full state feedback SEA control, deriving necessary and sufficient passivity conditions for the nominal model, a demonstration that the design model almost prohibits strict passivity, and finds sufficient conditions for relaxed passivity in the nominal model.

REFERENCES

[1] G. A. Pratt and M. M. Williamson, "Series elastic actuators," in *Proc. 1995 IEEE/RSJ Int. Conf. Intelligent Robots and Systems*, vol. 1, pp. 399–406.

[2] M. W. Spong, "Modeling and control of elastic joint robots," *J. Dyn. Syst. Meas. Control*, vol. 109, no. 4, pp. 310–319, 1987.

[3] H. Vallery, R. Ekkelenkamp, H. Van Der Kooij, and M. Buss, "Passive and accurate torque control of series elastic actuators," in *Proc. 2007 IEEE/RSJ Int. Conf. Intelligent Robots and Systems*, pp. 3534–3538.

[4] A. Albu-Schäffer, C. Ott, and G. Hirzinger, "A unified passivity-based

control framework for position, torque and impedance control of flexible joint robots," *Int. J. Robotics Research*, vol. 26, no. 1, pp. 23–39, 2007.

[5] N. L. Tagliamonte, D. Accoto, and E. Guglielmelli, "Rendering viscoelasticity with series elastic actuators using cascade control," in *2014 IEEE Int. Conf. Robotics and Automation*, pp. 2424–2429.

[6] D. Kim, Y. Zhao, G. Thomas, B. R. Fernandez, and L. Sentis, "Stabilizing series-elastic point-foot bipeds using whole-body operational space control," *IEEE Trans. Robotics*, vol. 32, no. 6, pp. 1362–1379, 2016.

[7] N. Paine, J. S. Mehling, J. Holley, N. A. Radford, G. Johnson, C.-L. Fok, and L. Sentis, "Actuator control for the nasa-jsc valkyrie humanoid robot: A decoupled dynamics approach for torque control of series elastic robots," *J. Field Robotics*, vol. 32, no. 3, pp. 378–396, 2015.

[8] A. Albu-Schäffer and G. Hirzinger, "State feedback controller for flexible joint robots: A globally stable approach implemented on dlr's lightweight robots," in *Proc. 2000 IEEE/RSJ Int. Conf. Intelligent Robots and Systems*, vol. 2, pp. 1087–1093.

[9] ——, "Cartesian impedance control techniques for torque controlled light-weight robots," in *Proc. 2002 IEEE Int. Conf. Robotics and Automation*, vol. 1, pp. 657–663.

[10] A. Albu-Schäffer, C. Ott, and G. Hirzinger, "A passivity based cartesian impedance controller for flexible joint robots-part ii: Full state feedback, impedance design and experiments," in *Proc. 2004 IEEE Int. Conf. Robotics and Automation*, vol. 3, pp. 2666–2672.

[11] S. P. Boyd, L. El Ghaoui, E. Feron, and V. Balakrishnan, *Linear matrix inequalities in system and control theory*. SIAM, 1994.

[12] C. Ott, A. Albu-Schäffer, A. Kugi, and G. Hirzinger, "On the passivity–based impedance control of flexible joint robots," *IEEE Trans. Robotics*, vol. 24, no. 2, pp. 416–429, 2008.

[13] K. Isik, G. C. Thomas, and L. Sentis, "A fixed structure gain selection strategy for high impedance series elastic actuator behavior," *J. Dyn. Syst. Meas. Control*, vol. 141, no. 2, p. 021009, 2019.

[14] Y. Zhao, N. Paine, S. J. Jorgensen, and L. Sentis, "Impedance control and performance measure of series elastic actuators," *IEEE Trans. Ind. Electron.*, vol. 65, no. 3, pp. 2817–2827, 2018.

[15] K. Haninger and M. Tomizuka, "Robust passivity and passivity relaxation for impedance control of flexible-joint robots with inner-loop torque control," *IEEE/ASME Trans. Mechatronics*, vol. 23, no. 6, pp. 2671–2680, 2018.

[16] G. C. Thomas and L. Sentis, "MIMO identification of frequency-domain unreliability in SEAs," in *Proc. 2017 American Control Conference*. IEEE, pp. 4436–4441.

[17] ——, "Quadric inclusion programs: an lmi approach to $\mathcal{H}_\infty$-model identification," *IEEE Trans. Automatic Control*, vol. 64, no. 10, pp. 4229–4236, 2019.

[18] L. Le-Tien, A. Albu-Schäffer, and G. Hirzinger, "Mimo state feedback controller for a flexible joint robot with strong joint coupling," in *Proc. 2007 IEEE Int. Conf. Robotics and Automation*, pp. 3824–3830.

[19] F. Petit and A. Albu-Schäffer, "State feedback damping control for a multi dof variable stiffness robot arm," in *Proc. 2011 IEEE Int. Conf. Robotics and Automation*, pp. 5561–5567.

[20] L. Le-Tien and A. Albu-Schäffer, "Improving tracking accuracy of a mimo state feedback controller for elastic joint robots," in *53rd IEEE Conf. Decision and Control*, 2014, pp. 4548–4553.

[21] ——, "Decoupling and tracking control for elastic joint robots with coupled joint structure," *Adv. Robotics*, vol. 31, no. 4, pp. 184–203, 2017.

[22] L. Le-Tien, A. Albu-Schäffer, A. De Luca, and G. Hirzinger, "Friction observer and compensation for control of robots with joint torque measurement," in *Proc. 2008 IEEE/RSJ Int. Conf. Intelligent Robots and Systems*, pp. 3789–3795.

[23] T. Kawakami, K. Ayusawa, H. Kaminaga, and Y. Nakamura, "High-fidelity joint drive system by torque feedback control using high precision linear encoder," in *Proc. 2010 IEEE Int. Conf. Robotics and Automation*, pp. 3904–3909.

[24] M. J. Kim and W. K. Chung, "Disturbance-observer-based pd control of flexible joint robots for asymptotic convergence," *IEEE Trans. Robotics*, vol. 31, no. 6, pp. 1508–1516, 2015.

[25] M. J. Kim, F. Beck, C. Ott, and A. Albu-Schäffer, "Model-free friction observers for flexible joint robots with torque measurements," *IEEE Trans. Robotics*, vol. 35, no. 6, pp. 1508–1515, 2019.

[26] J. S. Mehling, J. Holley, and M. K. O'Malley, "Leveraging disturbance observer based torque control for improved impedance rendering with series elastic actuators," in *Proc. 2015 IEEE/RSJ Int. Conf. Intelligent Robots and Systems*, pp. 1646–1651.